A Marcus Treatment of Rate Constants for Protonation of Ring-Substituted α-Methoxystyrenes: Intrinsic Reaction Barriers and the Shape of the Reaction Coordinate

John P. Richard* and Kathleen B. Williams

Contribution from the Department of Chemistry, University at Buffalo, SUNY, Buffalo New York 14260-3000

Received February 12, 2007; E-mail: jrichard@chem.buffalo.edu

Abstract: Rate and equilibrium constants were determined for protonation of ring-substituted α-methoxy-styrenes by hydronium ion and by carboxylic acids to form the corresponding ring-substituted α-methyl α-methoxybenzyl carbocations at 25 °C and $I = 1.0$ (KCl). The thermodynamic barrier to carbocation formation increases by 14.5 kcal/mol as the phenyl ring substituent(s) is changed from 4-MeO- to 3,5-di-NO$_2$-, and as the carboxylic acid is changed from dichloroacetic to acetic acid. The Brønsted coefficient α for protonation by carboxylic acids increases from 0.67 to 0.77 over this range of phenyl ring substituents, and the Brønsted coefficient β for proton transfer increases from 0.63 to 0.69 as the carboxylic acid is changed from dichloroacetic to acetic acid. The change in these Brønsted coefficients with changing reaction driving force, $\partial\alpha/\partial\Delta G^{\circ}_{av} = \partial\beta/\partial\Delta G^{\circ}_{av} = 1/8\Lambda = 0.011$, is used to calculate a Marcus intrinsic reaction barrier of $\Lambda = 11$ kcal/mol which is close to the barrier of 13 kcal/mol for thermoneutral proton transfer between this series of acids and bases. The value of α = 0.66 for thermoneutral proton transfer is greater than α = 0.50 required by a reaction that follows the Marcus equation. This elevated value of β may be due to an asymmetry in the reaction coordinate that arises from the difference in the intrinsic barriers for proton transfer at the oxygen acid reactant and resonance-stabilized carbon acid product.

Introduction

Marcus theory provides a framework for treating kinetic data for electron-transfer reactions.[1] The Marcus eq 1, which is central to this theory, predicts a simple relationship between the activation barriers for electron transfer ($\Delta G^{\dagger}$) and the following quantities: (1) the thermodynamic driving force for the reaction (ΔG°), (2) the intrinsic activation barrier Λ when $\Delta G^{\circ} = 0$ for the chemical portion of the reaction, and (3) the work to bring reactants together into a reactive complex (ω_r) and the negative work done when the product complex separates to free products ($-\omega_p$). This equation predicts nonlinear logarithmic structure−reactivity relationships between rate and equilibrium constants for these reactions, and it has been applied by Marcus to simple organic reactions that exhibit such structure−reactivity correlations.[2,3] Marcus theory has been refined in attempts to model reaction coordinate profiles for complex chemical reactions,[4−6] and the simple Marcus equation has been used to rationalize rate data for a variety of organic reactions including proton transfer at carbon,[7−9] nucleophilic

addition to the carbonyl group[10,11] and to carbocations,[8,12] and bimolecular nucleophilic aliphatic substitution.[13,14]

$$\Delta G^{\dagger} = \omega_r + \Lambda\left(1 + \frac{\Delta G^{\circ} - \omega_r + \omega_p}{4\Lambda}\right)^2 \qquad (1)$$

$$\Delta G^{\dagger} = \Lambda\left(1 + \frac{\Delta G^{\circ}}{4\Lambda}\right)^2 \qquad (2)$$

$$\frac{\partial^2\Delta G^{\dagger}}{\partial^2\Delta G^{\circ}} = \frac{1}{8\Lambda} \qquad (3)$$

Organic reactions that involve extensive electronic reorganization and changes in bonding to the reacting atoms differ from the electron-transfer reactions that Marcus theory was developed to treat. The intrinsic barrier to electron transfer can be modeled as the barrier to reorganization of solvent required for optimal tunneling of an electron from the donor to acceptor groups; however, the intrinsic barrier to complex organic reactions is determined by the relative energies of the reactant state and a metastable transition state in which there are transient partial covalent bonds to one of more atoms. There are very difficult questions about the origin of the barrier to organic reactions that need to be addressed, but these questions have

(1) Marcus, R. A. *J. Chem. Phys.* **1956**, *24*, 966−978.
(2) Marcus, R. A. *J. Phys. Chem.* **1968**, *72*, 891−899.
(3) Marcus, R. A. *J. Am. Chem. Soc.* **1969**, *91*, 7224−7225.
(4) Chen, M. Y.; Murdoch, J. R. *J. Am. Chem. Soc.* **1984**, *106*, 4735−4743.
(5) Murdoch, J. R. *J. Am. Chem. Soc.* **1983**, *105*, 2660−2667.
(6) Guthrie, J. P. *J. Am. Chem. Soc.* **1996**, *118*, 12878−12885.
(7) Kresge, A. J. *Chem Soc. Rev.* **1973**, *2*, 475−503.
(8) Richard, J. P.; Amyes, T. L.; Toteva, M. M. *Acc. Chem. Res.* **2001**, *34*, 981−988.
(9) Guthrie, J. P. *J. Am. Chem. Soc.* **1997**, *119*, 1151−1152.

(10) Guthrie, J. P.; Pitchko, V. *J. Am. Chem. Soc.* **2000**, *122*, 5520−5528.
(11) Guthrie, J. P. *J. Am. Chem. Soc.* **2000**, *122*, 5529−5538.
(12) Guthrie, J. P.; Pitchko, V. *J. Phys. Org. Chem.* **2004**, *17*, 548−559.
(13) Albery, W. J.; Kreevoy, M. M. *Adv. Phys. Org. Chem.* **1978**, *16*, 87−157.
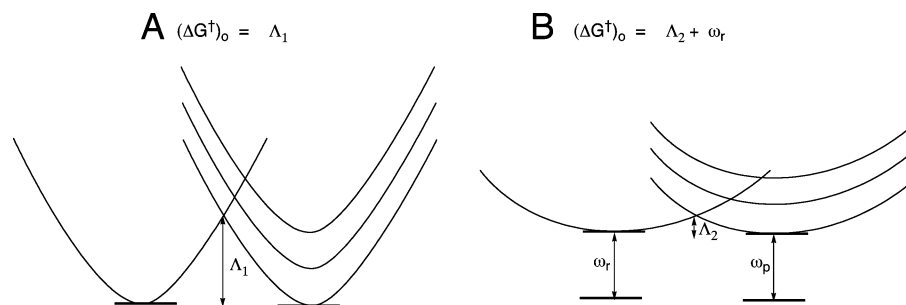(14) Lewis, E. S.; Hu, D. C. *J. Am. Chem. Soc.* **1984**, *106*, 3292−3296.

Figure 1. (A) Free-energy profile for a reaction where the work term $\omega_r = 0$, the observed barrier for the thermoneutral reaction is equal to the intrinsic reaction barrier, and a minimum shift in the position of the reaction transition state with changing reaction driving force is observed. (B) Free-energy profile for a reaction where there is a large work term ω_r, the observed barrier for the thermoneutral reaction is much larger than the intrinsic reaction barrier, and a substantial shift in the position of the reaction transition state with changing reaction driving force is observed.

not seriously discouraged the use of Marcus theory to describe experimental rate−equilibrium data. We have followed the lead of Bernasconi and co-workers[15−18] and have shown that the systematic changes observed in the intrinsic barriers for a broad range of proton transfer and carbocation−nucleophile combination reactions provide considerable insight into the factors that affect the stability of the transition states for these reactions.[8]

The Marcus intrinsic reaction barrier may be estimated as the activation barrier for a formally thermoneutral reaction by assuming that $\omega_r = \omega_P = 0$. In this case, the reactant complex will not differ greatly from free reactants, and the observed activation barrier will be equal to the change in the energy of the reactant complex that occurs on moving to the transition state. A significant work term is sometimes used when fitting kinetic data to the Marcus equation, but to the best of our knowledge there have been no systematic attempts in earlier studies to partition an observed reaction barrier into *work* done in formation of a complex between reactants, and the change in energy as this complex moves to the reaction transition state. Uncertainty in the significance of this work term has led to reports of very different values of Λ for similar proton-transfer reactions at α-methyl ketones and O-alkylated α-methyl ketones.[19−21]

The *intrinsic* barrier Λ for a chemical reaction defines the steepness of curvature of the reaction coordinate, and this, in turn, determines the sensitivity of the position of the reaction transition to changes in thermodynamic driving force. A large, formal intrinsic barrier Λ requires a reaction coordinate with a steep ascent to a transition state whose position will shift only slightly with changing reaction driving force (Figure 1A). The steepness of the ascent to the transition state decreases with decreasing Λ, and this will lead to a sharper shift in the position of the transition state with changing reaction driving force (Figure 1B).

The magnitude in the shift of the position of the transition state with changing thermodynamic driving force can be evaluated by determining the appropriate second-derivative structure−reactivity coefficient.[7] In the case of proton-transfer reactions, the approximate position of the transition state is defined by the Brønsted coefficient, $\alpha = \partial \log k_{HA}/\partial pK_{HA}$, where k_{HA} is the second-order rate constant for proton transfer

Scheme 1

X = 4-OMe, H, 4-NO$_2$, 3,5-di-NO$_2$
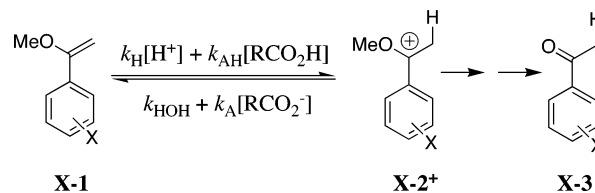
and K_{HA} is the acidity constant of the Brønsted acid. The magnitude of the shift in the position of the transition state ($\partial\alpha$) with changing thermodynamic driving force for the reaction (∂pK_{BH}, where pK_{BH} is the pK_a of the conjugate acid of the reacting base) is a second-derivative structure−reactivity effect. This effect is equal to the second derivative of the Marcus equation and is inversely proportional to the intrinsic barrier Λ (eq 3).[7,22,23] The difference between the observed barrier for a thermoneutral reaction and the Marcus intrinsic barrier estimated from an analysis of the second derivative structure−reactivity effect provides an estimate for the work term ω_r.

We report here a complete set of rate and equilibrium constants for reversible protonation of ring-substituted α-methoxystyrenes (**X-1**) by hydronium ion and by substituted carboxylic acids to form the corresponding oxocarbenium ions (Scheme 1). This set of data is used to estimate the intrinsic reaction barrier Λ from the second-derivative structure−reactivity term: $\partial^2 \log \Delta G^\ddagger/\partial(\Delta G°)_{HA}\partial(\Delta G°)_{HB} = 1/8\Lambda$.[7] The value of Λ calculated from this structure−reactivity analysis is similar to the observed activation barrier to thermoneutral proton transfer. This provides evidence that little work is performed on moving from free reactants to the complex that undergoes the proton-transfer reaction. These data also reveal deviations from *ideal* Marcus behavior that are pertinent to the use of the Marcus equation as a descriptor of the reaction coordinate profile for organic reactions.

Experimental Section

Solvents were used without further purification unless otherwise indicated. Water was first distilled and then further purified with a Milli-Q water apparatus. Deuterated solvents were purchased from Cambridge Isotope Laboratories. Methanol and acetonitrile from Fisher were HPLC grade, and all other solvents used for chemical syntheses were reagent grade.

(15) Bernasconi, C. F. *Tetrahedron* **1985**, *41*, 3219−3234.
(16) Bernasconi, C. F. *Acc. Chem. Res.* **1987**, *20*, 301−308.
(17) Bernasconi, C. F. *Acc. Chem. Res.* **1992**, *25*, 9−16.
(18) Bernasoni, C. F. *Adv. Phys. Org. Chem.* **1992**, *27*, 119−238.
(19) Gerlt, J. A.; Gassman, P. G. *J. Am. Chem. Soc.* **1993**, *115*, 11552−11568.
(20) Guthrie, J. P. *J. Am. Chem. Soc.* **1991**, *113*, 7249−7255.
(21) Toullec, J. *J. Chem. Soc., Perkin Trans. 2* **1989**, 167−171.

(22) Jencks, W. P. *Bull. Chim. Soc. France* **1988**, 218−224.
(23) Richard, J. P.; Amyes, T. L.; Vontor, T. *J. Am. Chem. Soc.* **1992**, *114*, 5626−5634.

The following organic compounds were reagent grade from Aldrich and were used without further purification: 3,5-dinitrobenzoyl chloride (≥98%), 4-methoxyacetophenone (99%), acetophenone (99%), 4-nitroacetophenone (98%), trimethylorthoformate (>99%), *p*-toluenesulfonic acid monohydrate (99%), sodium carbonate, potassium acetate (>99%), potassium phosphate (dibasic trihydrate, 99+%), potassium phosphate (monobasic, 99%), methoxyacetic acid (98%), cyanoacetic acid (>99%), and dichloroacetic acid (>99%). Choloroacetic acid (>99%) was recrystallized from chloroform. Acetophenone dimethyl ketal used in product studies was purified by preparative HPLC to remove small amounts of alkene and ketone impurities. [2-*N*-Morpholino]ethanesulfonic acid (MES, 99.5%) was purchased from Sigma. 3,5-Dinitroacetophenone was prepared from 3,5-dinitrobenzoyl chloride and diethylmagnesium malonate by following a published procedure.[24]

^{1}H NMR spectra were obtained on a Varian Gemini 300, a UNITY INOVA 400, or a UNITY INOVA 500 MHz NMR spectrometer. ^{1}H NMR spectra were obtained using CDCl$_3$ as the solvent unless otherwise stated. Chemical shifts (ppm) were determined using tetramethylsilane (TMS) as an internal reference at zero ppm. High performance liquid chromatography (HPLC) was performed using a system described in earlier work.[25,26] Measurements of pH were obtained using a Ross Combination pH electrode from Orion or a Radiometer Combination pH electrode.

Syntheses. The procedures for the synthesis of the following compounds, along with spectroscopic data and analytical data, are given in the Supporting Information: 4-methoxyacetophenone dimethyl ketal, 4-nitroacetophenone dimethyl ketal, 3,5-dinitroacetophenone dimethyl ketal, α-methoxy-4-methoxystyrene, α-methoxystyrene, α-methoxy-4-nitrostyrene, and α-methoxy-3,5-dinitrostyrene.

Kinetic Studies. Reactions were performed in buffered solutions of H$_2$O at 25 °C with the ionic strength maintained at 1.0 (KCl). The reactions were initiated by making a 1/100 dilution of the substrate in acetonitrile to give the following final concentrations: α-methoxy-4-methoxystyrene, 0.05 mM; α-methoxystyrene, 0.5 mM; α-methoxy-4-nitrostyrene, 5 μM; α-methoxy-3,5-dinitrostyrene, 0.02 mM. The substrate solution in acetonitrile used in kinetic analyses by HPLC contained 2 mM 9-hydroxy-9 methylfluorene as an internal standard that was used to correct for small errors in injection volume. The hydrolysis reaction of **X-1** (X = 4-OMe, H, 4-NO$_2$) was followed spectrophotometrically by monitoring the change in absorbance at the following wavelengths: **4-MeO-1**, 267 nm; **H-1**, 245 or 269 nm; and **4-NO$_2$-1**, 268 nm. The slow reaction of **3,5-di-NO$_2$-1** was monitored by separation of the product ketone from the substrate by HPLC, with peak detection at 250 nm.

Literature values for the pK_a's of the carboxylic acids used in this work are for ionization at $I = 1.0$ (KCl).[27] For reactions at pH within one unit of the pK_a of the carboxylic acid catalyst, the solutions of substrate were prepared by making the appropriate dilution of a 1.0 M solution of the buffer catalyst ($I = 1.0$, KCl) with 1.0 M KCl. In many cases catalysis by Brønsted acids was examined at pH > pK_a, using [2-*N*-morpholino]ethanesulfonic acid (MES, pK_a = 6.5) to maintain constant pH. These solutions were prepared by mixing a 0.5 M solution of the MES buffer ($I = 1.0$, KCl) with the carboxylic acid catalyst at the same pH and ionic strength and diluting the resulting solution with 1.0 M KCl to give a final MES concentration of 20 mM and final concentrations of 0.05−0.50 M for {[RCO$_2$H + RCO$^-$]}. The pH of the solution was determined at the beginning and upon completion of the kinetic experiment, and the change in pH was found in all cases to be ≤0.05 units.

$$\left(\frac{[P]}{[S]_0}\right) = \left(\frac{A_P}{(A_S)_0}\right)\left(\frac{\epsilon_S}{\epsilon_P}\right) \tag{4}$$

$$\left(\frac{[\text{alkene}]}{[\text{ketone}]}\right) = \left(\frac{A_{\text{alk}}}{A_{\text{ket}}}\right)\left(\frac{\epsilon_{\text{ket}}}{\epsilon_{\text{alk}}}\right) \tag{5}$$

Values of the first-order rate constants (k_{obsd}) for the reactions of **4-MeO-1**, **H-1**, and **4-NO$_2$-1** were determined as the slopes of linear semilogarithmic plots of reaction progress against time. The reactions obeyed first-order kinetics for more than three reactions halftimes, and the values of k_{obsd} were reproducible to ±5%. Rate constants for the reactions of **3,5-di-NO$_2$-1** at pH > 4.6 were determined using the method of initial rates by monitoring the initial conversion of ≤6% of reactant to product and using HPLC to separate the reactant from product. The values of k_{obsd} were determined as the slopes of linear plots of [P]/[S]$_0$ against time, where [P] and [S]$_0$ are the concentration of the product and the initial concentration of the substrate, respectively. The values of [P]/[S]$_0$ were determined from the peak areas of the product, A_P, and the initial peak area of the substrate at $t = 0$, $(A_S)_0$ at 250 nm (eq 4), where $\epsilon_S/\epsilon_P = 1.44$ is the ratio of the extinction coefficients of the substrate and product at 250 nm determined by HPLC analysis of known amounts of these compounds. Second-order rate constants k_{HA} for general acid catalysis were determined as the slopes of linear plots of $k_{\text{obsd}}/[\text{H}^+]$ against [HA]/[H$^+$]. The values of k_{HA} determined in wholly separate experiments agree to better than ±10%.

Products of Solvolysis of Acetophenone Dimethyl Ketal. The solvolysis of acetophenone dimethyl ketal to form the alkene and ketone products was initiated by making a 100-fold dilution of a 0.15 M solution of the ketal in acetonitrile that contained 0.5 mM fluorene into water buffered with phosphate at pH 7.0. The products were separated by HPLC, eluting with methanol/water that contained 10 mM carbonate buffer at pH 9 and with peak detection at 269 nm. The ratio of the product yields was determined from the ratio of the HPLC peak areas $A_{\text{alk}}/A_{\text{ket}}$ using eq 5, and $\epsilon_{\text{ket}}/\epsilon_{\text{alk}} = 0.46$ for the ratio of the extinction coefficients of the acetophenone and α-methoxystyrene products. The second ratio was determined by HPLC analysis of known amounts of these two compounds. The product ratio [alkene]/[ketone] decreased slowly with time, due to acid-catalyzed conversion of the alkene the acetophenone. The initial ratio of product yields was determined by making a small (<20%) linear extrapolation to zero time of a plot of $A_{\text{alk}}/A_{\text{ket}}$ against time.

Results

The reactions of ring-substituted α-methoxystyrenes **X-1** to form the corresponding ring-substituted acetophenone **X-3** were monitored by UV spectroscopy. In all cases the kinetic data can be fit to the rate law for a first-order reaction. This is consistent with a large body of data which shows that protonation of the alkene to form **X-2**$^+$ is the rate-determining step for the reaction shown in Scheme 1.[28−30] Tables S1−S7 in the Supporting Information report the observed first-order rate constants for the reactions of **X-1** that were used to determine the second-order rate constants for the reactions catalyzed by Brønsted general acids and by the hydrogen ion.

The values of the first-order rate constants k_o for the reactions of **4-NO$_2$-1** and **3,5-di-NO$_2$-1** were determined for reactions at five different concentrations of hydronium ion between 0.01 and 0.05 M (Table S7). Figure 2 shows these data plotted as logarithmic pH rate profiles. The α-methoxystyrenes **H-1** and **4-MeO-1** are too reactive to conveniently study in unbuffered acidic solutions ($-\log[\text{H}^+] \leq 3$). The observed first-order rate constants for hydrolysis of these vinyl ethers

(24) Alpha, S. R. *J. Org. Chem.* **1973**, *38*, 3136−3139.
(25) Toteva, M. M.; Moran, M.; Amyes, T. L.; Richard, J. P. *J. Am. Chem. Soc.* **2003**, *125*, 8814−8819.
(26) Tsuji, Y.; Toteva, M. M.; Garth, H. A.; Richard, J. P. *J. Am. Chem. Soc.* **2003**, *125*, 15455−15465.
(27) Fox, J. P.; Jencks, W. P. *J. Am. Chem. Soc.* **1974**, *96*, 1436−1449.

(28) Kresge, A. J.; Chen, H.-L.; Chiang, Y.; Murrill, E.; Payne, M. A.; Sagatys, D. S. *J. Am. Chem. Soc.* **1971**, *93*, 413−423.
(29) Kresge, A. J.; Sagatys, D. S.; Chen, H. L. *J. Am. Chem. Soc.* **1977**, *99*, 7228−7233.
(30) Loudon, G. M.; Smith, C. K.; Zimmerman, S. E. *J. Am. Chem. Soc.* **1974**, *96*.
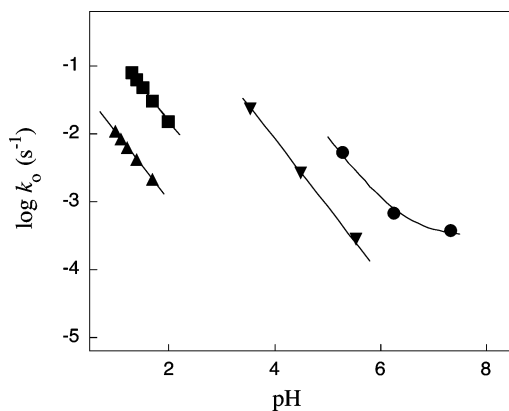
Figure 2. pH-rate profiles for the hydrolysis of ring-substituted α-methoxystyrenes **X-1** at 25 °C and $I = 1.0$ (KCl). Key: (●): Hydrolysis of **4-MeO-1**. (▼): Hydrolysis of **H-1**. (◆): Hydrolysis of **4-NO₂-1**. (▲): Hydrolysis of **3,5-di-NO₂-1**.

Table 1. Second-Order Rate Constants for Acid-Catalyzed Hydrolysis of **X-1** in Water at 25 °C and $I = 1.0$ (KCl)

	k_{HA} (M^{-1} s^{-1})^b			
catalyst (pK_a)^a	4-MeO-1	H-1	4-NO₂-1	3,5-di-NO₂-1
HOH^c (15.7)	3.1×10^{-4} $\pm 6 \times 10^{-5}$ ^{e,f}			
CH₃CO₂H^d (4.60)	2.0	0.13	1.2×10^{-3}	6.6×10^{-5}
CH₃OCH₂CO₂H^d (3.33)	18	1.0	9.5×10^{-3}	7.4×10^{-4}
ClCH₂CO₂H^d (2.65)	45	3.9	4.6×10^{-2}	2.3×10^{-3}
NCCH₂CO₂H^d (2.23)	59	5.3	6.2×10^{-2}	2.7×10^{-3}
Cl₂CHCO₂H^d (1.03)	570	60	0.72	4.7×10^{-2}
H₃O$^{+\,c}$	$870 \pm 150^{e,f}$	85 ± 5^f	1.5 ± 0.014^f	0.105 ± 0.0013^f

^{a} Reference 27. ^{b} Second-order rate constant for acid-catalyzed hydrolysis of **X-1** to form the corresponding ketone. Protonation of **1-X** is the rate-determining step for the hydrolysis reaction.[27–30] ^{c} Determined from the fit of the data from Figure 2 to a logarithmic form of eq 6. ^{d} Determined from the fit of the experimental data to eq 7. ^{e} (s^{-1}). ^{f} Standard deviation from nonlinear least-squares analysis of the data shown in Figure 2.

were determined at near neutral pH in solutions buffered with [2-*N*-morpholino]ethanesulfonic acid (MES) [Tables S5 and S6]. The plots (not shown) of k_{obsd} against buffer concentration were linear and the rate constants k_o (s^{-1}) for the buffer-independent reactions were determined by extrapolating these linear plots to [B] = 0. These rate data are also plotted in logarithmic form in Figure 2. The value of k_H (M^{-1} s^{-1}) for the reaction of **H-1**, calculated from the fit of the data in Figure 2 to a logarithmic form of eq 6 ($k_w = 0$), is reported in Table 1. The upward break at high pH in the pH rate profile for the reaction of **4-MeO-1** shows that protonation by water is the dominant reaction pathway at high pH. Values of $k_H = 870$ M^{-1} s^{-1} and $k_w = 3.1 \times 10^{-4}$ s^{-1} were determined from the nonlinear least-squares fit of data from Figure 2 to a logarithmic form of eq 6 (Table 1).

$$k_o = k_w + k_H[H^+] \qquad (6)$$

$$k_{obsd}/[H^+] = k_o/[H^+] + k_{HA}([HA]/[H^+]) \qquad (7)$$

The α-methoxystyrene **4-MeO-1** is too reactive toward specific acid catalysis to conveniently study at pH = pK_a of alkane carboxylic acid buffer catalysts. These reactions were studied at pH ≫ pK_a in solutions buffered by MES. The values of k_{obsd} determined at increasing [RCO₂H] are summarized in Table S1 of the Supporting Information. Figure 3A shows the linear increase in $k_{obsd}/[H^+]$ for hydrolysis of **4-MeO-1** in the presence of increasing [CH₃COOH] at pH 6.6 (20 mM MES), 25 °C, and $I = 1.0$ KCl; Figure 4A shows the linear increase in $k_{obsd}/[H^+]$ for hydrolysis of **4-MeO-1** at increasing initial [Cl₂CHCOOH] at pH 6.7 (20 mM MES), 25 °C, and $I = 1.0$ KCl. Values of $k_{obsd}/[H^+]$ instead of simply k_{obsd} are plotted on the *y*-axes of Figures 3 and 4 in order to correct for the effect on k_{obsd} of the small (≤0.1 unit) change in the
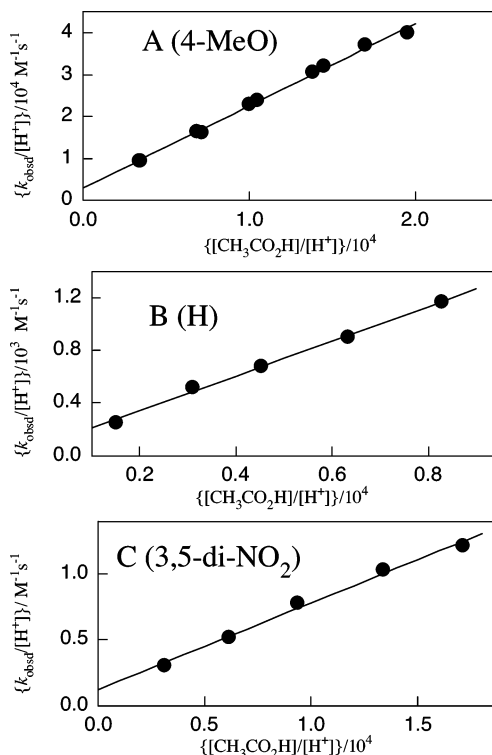

Figure 3. Effect of increasing [CH₃CO₂H] on the observed first-order rate constant, k_{obsd}, for hydrolysis of **X-1** at 25 °C and $I = 1.0$ (KCl). (A) Hydrolysis of **4-MeO-1** at pH 6.6 (20 mM MES). (B) Hydrolysis of **H-1** at pH 5.7 (20 mM MES). (C) Hydrolysis of **3,5-di-NO₂-1** at pH 5.6 (20 mM MES).
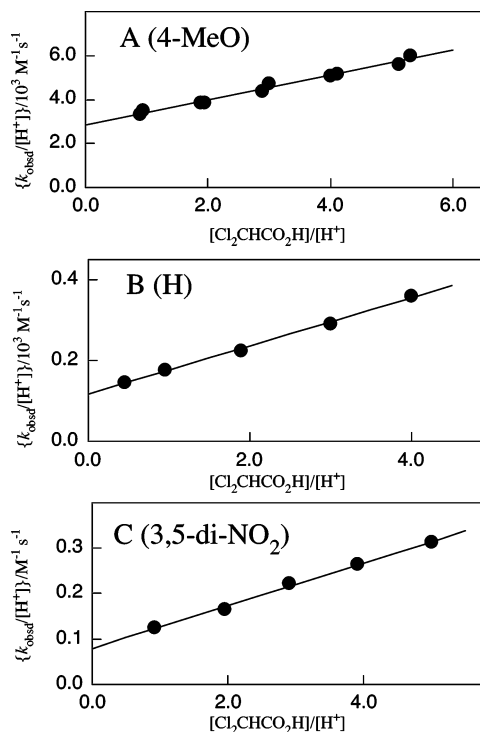

Figure 4. Effect of increasing [CHCl₂CO₂H] on the observed first-order rate constants, k_{obsd} for hydrolysis of **X-1** at 25 °C and $I = 1.0$ (KCl). (A) Hydrolysis of **4-MeO-1** at pH 6.7 (20 mM MES). (B) Hydrolysis of **H-1** at pH 5.6 (20 mM MES). (C) Hydrolysis of **3,5-di-NO₂-1** at pH 5.7 (20 mM MES).

initial pH sometimes observed as {[RCO₂H] + [RO₂$^-$]} is increased to 0.50 M (Tables S1–S4). Values for the second-order rate constants k_{HA} for general acid catalysis of the hydrolysis reactions of **4-MeO-1**,

Table 2. Equilibrium Constants for the Interconversion of **X-1**, **X-2**$^+$, and the Corresponding Dimethyl Ketal (Schemes 1 and 3), Rate Constants for the Reversible Protonation of **X-1**, and the Change in Gibbs Free Energy for This Reaction in Water at 25 °C and $I = 1.0$ (KCl)

ring substituent	equilibrium constant[a]				acid catalyst					
	K_{alk}/M^{-1}[b]	$(pK_R)_{MeOH}$[c]	$(pK_a)_{ox}$[d]	$\log k$[e]	H$^+$	Cl$_2$CHCO$_2$H	CNCH$_2$CO$_2$H	ClCH$_2$CO$_2$H	MeOCH$_2$CO$_2$H	CH$_3$CO$_2$H
4-MeO-	13	−0.81	0.30	$k_{HA}/M^{-1}\,s^{-1}$[f]	2.94	2.76	1.77	1.65	1.26	0.30
				$k_A/M^{-1}\,s^{-1}$[g]	2.6[h]	3.49	3.70	4.0	4.28	4.60
				$\Delta G°$/kcal/mol	−2.8[i]	1.0	2.6	3.2	4.1	5.8
H	17	−2.7	−1.5	$k_{HA}/M^{-1}\,s^{-1}$[f]	1.93	1.78	0.72	0.59	0.00	−0.89
				$k_A/M^{-1}\,s^{-1}$[g]	3.4[h]	4.3	4.5	4.7	4.8	5.2
				$\Delta G°$/kcal/mol	−0.4[i]	3.4	5.1	5.6	6.6	8.3
4-NO$_2$	25	−5.5	−4.1	$k_{HA}/M^{-1}\,s^{-1}$[f]	0.176	−0.143	−1.21	−1.34	−2.02	−2.92
				$k_A/M^{-1}\,s^{-1}$[g]	4.3[h]	5.0	5.2	5.4	5.4	5.8
				$\Delta G°$/kcal/mol	3.2[i]	7.0	8.6	9.2	10.1	11.9
3,5-di-NO$_2$	34	−7.8	−6.3	$k_{HA}/M^{-1}\,s^{-1}$[f]	−0.98	−1.33	−2.57	−2.64	−3.13	−4.18
				$k_A/M^{-1}\,s^{-1}$[g]	5.3[h]	6.0	5.9	6.3	6.5	6.7
				$\Delta G°$/kcal/mol	6.2[i]	10	11.6	12.2	13.1	14.8

[a] Equilibrium constants defined in Scheme 3. [b] Data from ref 21. The value of K_{alk} for hydration of **3,5-di-NO$_2$-1** was estimated using the Hammett equation, $\rho_{alk} = 0.21$ calculated from the values of K_{alk} for hydration of **H-1** and **4-NO$_2$-1** ($\sigma_{NO2} = 0.78$) and $\sigma = 2(0.71) = 1.42$ for the **3,5-di-NO$_2$**-substituents [ref 35]. [c] See text. [d] $(pK_a)_{oxo} = (pK_R)_{MeOH} + \log K_{alk}$. [e] Rate constants and the change in standard Gibbs free energy for the conversion of **X-1** to **X-2**$^+$. [f] Rate constants from Table 1. [g] Calculated from the values of $(K_a)_{ox}$ and k_{HA} using eq 10. [h] First-order rate constant (s^{-1}). [i] Calculated for a dimensionless equilibrium constant determined using a standard state concentration of 1.0 M for the proton-transfer reaction.

determined from the linear least-squares fit of the data to eq 7, are reported in Table 1.

Brønsted general acid catalysis of the hydrolysis of **3,5-di-NO$_2$-1** was studied at pH 5.6 (20 mM MES), $I = 1.0$ (KCl) and 25 °C. The observed first-order rate constants determined for these reactions are reported in Table S4. Figure 3C shows the linear increase in $k_{obsd}/[H^+]$ for hydrolysis of **3,5-di-NO$_2$-1** in the presence of increasing [CH$_3$COOH]; and, Figure 4C shows the linear increase in $k_{obsd}/[H^+]$ for hydrolysis of **3,5-di-NO$_2$-1** in the presence of increasing [Cl$_2$CHCOOH]. Values for the second-order rate constants k_{HA} (Table 1) for general acid catalysis of the hydrolysis of **3,5-di-NO$_2$-1**, determined from the linear least-squares fit of the data to eq 7, are reported in Table 1.

The observed first-order rate constants determined for buffer-catalyzed hydrolysis of **H-1** are reported in Table S2. Figure 3B shows the linear increase in $k_{obsd}/[H^+]$ for hydrolysis of **H-1** in the presence of increasing [CH$_3$CO$_2$H] at pH 5.7 (20 mM MES), 25 °C, and $I = 1.0$ KCl. Figure 4B shows the linear increase in $k_{obsd}/[H^+]$ for hydrolysis of **1** in the presence of increasing [Cl$_2$CHCO$_2$H] at pH 5.6 (20 mM MES), 25 °C, and $I = 1.0$ KCl. Values for the second-order rate constants k_{HA} for general acid catalysis of the hydrolysis reactions of **H-1**, determined from the linear least-squares fit of the data to eq 7, are reported in Table 1. The second-order rate constants for the hydrolysis of **H-1** catalyzed by other alkane carboxylic acids are reported in Table 1.

The observed first-order rate constants determined for buffer-catalyzed hydrolysis of **4-NO$_2$-1** are reported in Table S3. Table 1 reports values of k_{HA} (M^{-1} s^{-1}) for general acid-catalyzed hydrolysis of **4-NO$_2$-1** determined from the linear least-squares fit of plots of $k_{obsd}/[HA]/[H^+]$ against [HA]/[H$^+$]. The hydrolysis reactions of **4-NO$_2$-1** catalyzed by acetic acid and methoxyacetic acid were studied using these carboxylic acid catalysts as buffers. The hydrolysis reactions catalyzed by chloroacetic acid and by cyanoacetic acid were studied in solutions that contain 20 mM MES buffer ($I = 1.0$, KCl) at pH 4.8 and 4.3, respectively, where MES is a weak buffer. The reactions catalyzed by dichloroacetic acid were studied in solutions buffered with acetic acid ($I = 1.0$, KCl) at pH 4.1.

The second-order rate constant for the hydronium ion-catalyzed reaction of acetophenone dimethyl ketal ($k_H = 1600$ M^{-1} s^{-1})[31] is ∼20-fold larger than the rate constant for hydronium ion-catalyzed hydrolysis of the alkene **H-1** (Table 1). Therefore, it was possible to determine the yield of **H-1** that forms during the early stages of the reaction of
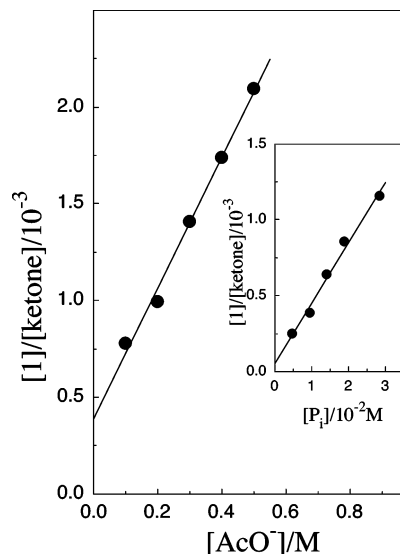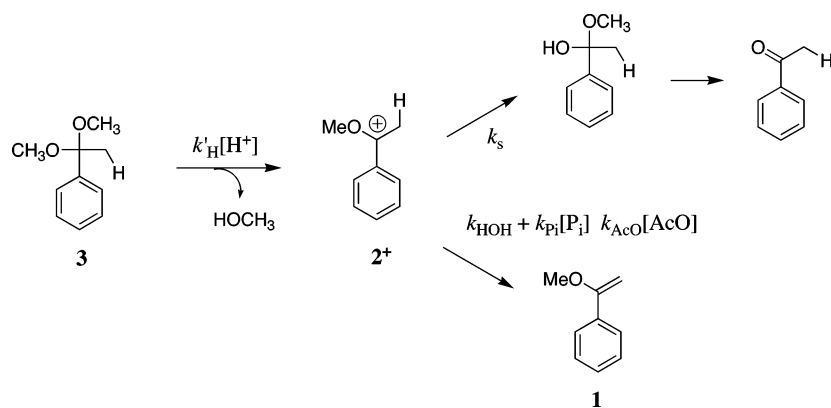
(31) Young, P. R.; Jencks, W. P. *J. Am. Chem. Soc.* **1977**, *99*, 8238−8248.

Figure 5. Effect of increasing the concentration of acetate ion on the ratio of the yields of **H-1** and acetophenone, [**H-1**]/[ketone], from the acid-catalyzed cleavage of acetophenone dimethyl ketal at pH 7.0 (10 mM phosphate buffer) in water at 25 °C and $I = 1.0$ (KCl). The solid line shows the least-squares fit of the data to eq 8. (Inset) Effect of increasing the concentration of phosphate buffer on [**H-1**]/[ketone]. The solid line shows the least-squares fit of the data to eq 8 ([AcO$^-$] = 0 M).

this ketal (Scheme 2). A small, 10−20% decrease in the ratio of the yields of **H-1** and acetophenone determined by HPLC analysis was observed during the first ∼30% of the specific acid-catalyzed hydrolysis of acetophenone dimethyl ketal at pH 7.0 (10 mM phosphate buffer and $I = 1.0$, KCl) and 25 °C. The initial product ratios [**H-1**]/[ketone] were determined by making short extrapolations to zero time for linear plots of [**H-1**]/[ketone] against time.

Figure 5 shows the effect of increasing the concentration of acetate ion on the ratio of the yields of **H-1** and acetophenone from specific acid-catalyzed hydrolysis of acetophenone dimethyl ketal in water at pH 7.0 (10 mM phosphate buffer), 25 °C, and $I = 1.0$, KCl. There should be little or no Brønsted general base catalysis of addition of water to **H-2**$^+$ because (1) There is no significant Brønsted acid catalysis of cleavage of the acetophenone dimethyl ketal or Brønsted base catalysis of addition of methanol to **H-2**$^+$ in the microscopic reverse direction.[31] (2) General base catalysis of addition of the water or the

Scheme 2

basic alcohols ethanol and methanol to the related ring-substituted 1-phenylethyl carbocations is weak or negligible.[32,33]

The data in Figure 5 were fit to eq 8, derived for Scheme 2 ([P_i] = 0.010 M), to give a slope of $k_{AcO}/k_s = 0.0034$ M^{-1}. The inset in Figure 5 shows the effect of increasing the concentration of phosphate buffer on [**H-1**]/[acetophenone], the products of specific acid-catalyzed cleavage of acetophenone dimethyl ketal at pH 7.0 in water at 25 °C and $I = 1.0$ (KCl). These data were fit to eq 8 ([AcO$^-$] = 0 M) to give a slope and intercept of $k_{Pi}/k_s = 0.040$ M^{-1} and $k_{HOH}/k_s = 5.5 \times 10^{-5}$, respectively.

$$\frac{[\mathbf{H}-\mathbf{1}]}{[\text{ketone}]} = \frac{k_{HOH}}{k_s} + \frac{k_{Pi}[P_i]}{k_s} + \frac{k_{AcO}[AcO]}{k_s} \qquad (8)$$

$$\frac{k_H}{k_{HA}} = \frac{k_{HOH}}{k_A K_a} \qquad (9)$$

Equation 9 is the relationship between rate constants for protonation of **H-1** and for deprotonation of **H-2$^+$** in the reverse direction (Scheme 1), where K_a is the acidity constant for the Brønsted acid. The value of $k_H/k_{HA} = 650$ calculated from the rate constants for the reaction of **H-1** (Table 1) is in good agreement with $k_{HOH}/k_A K_a = 640$ calculated from the values of $K_a = 10^{-4.6}$; $k_{HOH}/k_A = [(5.5 \times 10^{-5})/k_s]/[(3.4 \times 10^{-3}$ M$^{-1})/k_s] = 0.016$, determined from the fits of data shown in Figure 5. This agreement between rate constant ratios for catalysis of proton transfers in the forward and microscopic reverse directions shows that the rate constants determined in this work are internally consistent.

The following procedure was used in combining data reported here with data from earlier studies[21,31] in order to obtain the complete set of rate and equilibrium constants for Scheme 3 reported in Table 2.

(1) Values for the absolute rate constants for deprotonation of **H-2$^+$** by water ($k_{HOH} = 2750$ s^{-1}) and acetate ion ($k_A = 1.64 \times 10^5$ M^{-1} s^{-1}) were calculated from the values of the partition rate constant ratios (above) and $k_s = 1 \times 10^7$ s^{-1} for addition of water to **H-2$^+$**.[34]

(2) The (pK_a)$_{oxo}$ of -1.5 for **H-2$^+$** was calculated as log(k_{HOH}/k_H) = 2750 M^{-1} s^{-1}/85 M^{-1} s^{-1} for deprotonation of **H-2$^+$** and for protonation of **1** by hydronium ion (Table 1).

(3) The (pK_R)$_{MeOH}$ of -2.7 for the addition of methanol to **H-2$^+$** to form the dimethyl ketal and H$^+$ was calculated for Scheme 3 from the values of $K_{alk} = 17$,[21] (pK_a)$_{oxo} = -1.5$ (above), and (pK_R)$_{MeOH}$ = (pK_a)$_{oxo}$ − log K_{alk}.

(4) The (pK_R)$_{MeOH}$ of -0.81 for addition of methanol to **4-MeO-2$^+$** was calculated from (pK_R)$_{MeOH} = -2.7$ for the reaction of **H-2$^+$** and the 80-fold difference in the equilibrium constants for addition of methanol to **4-MeO-2$^+$** and **H-2$^+$** reported in earlier work.[31]

(32) Richard, J. P.; Jencks, W. P. *J. Am. Chem. Soc.* **1984**, *106*, 1396−1401.
(33) Ta-Shma, R.; Jencks, W. P. *J. Am. Chem. Soc.* **1986**, *108*, 8040−8050.
(34) Amyes, T. L.; Jencks, W. P. *J. Am. Chem. Soc.* **1989**, *111*, 7888−7900.

(5) The (pK_a)$_{oxo}$ of 0.30 for deprotonation of **4-MeO-2$^+$** was calculated for Scheme 3 from $K_{alk} = 13$,[21] (pK_R)$_{MeOH} = -0.81$, and (pK_a)$_{oxo}$ = (pK_R)$_{MeOH}$ + log K_{alk}.

(6) The values of (pK_R)$_{MeOH}$ for the addition of methanol to **4-NO$_2$-2$^+$** and to **3,5-di-NO$_2$-2$^+$** were calculated using the Hammett equation, (pK_R)$_{MeOH} = -2.7$ for the reaction of **H-2$^+$**,[31] the Hammett reaction constant $\rho = 3.6$ for addition of methanol to **X-1**,[31] and the Hammett substituent constants $\sigma = 0.78$ for **4-NO$_2$** and $\sigma = 2(0.71) = 1.42$ for **3,5-di-NO$_2$**.[35]

(7) The values of (pK_a)$_{oxo}$ for deprotonation of **4-NO$_2$-2$^+$** and **3,5-di-NO$_2$-2$^+$** were calculated for Scheme 3 from the values of K_{alk} and (pK_R)$_{MeOH}$ (Table 2) and the relationship (pK_a)$_{oxo}$ = (pK_R)$_{MeOH}$ + log K_{alk}.

(8) The values of the absolute rate constants k_A for deprotonation of **X-2$^+$** were calculated from (K_a)$_{oxo}$ and k_{HA} or k_H using eq 10 derived for Scheme 1.

$$(K_a)_{oxo} = \frac{k_{HOH}}{k_H} = \frac{k_A K_a}{k_{HA}} \qquad (10)$$

Scheme 3
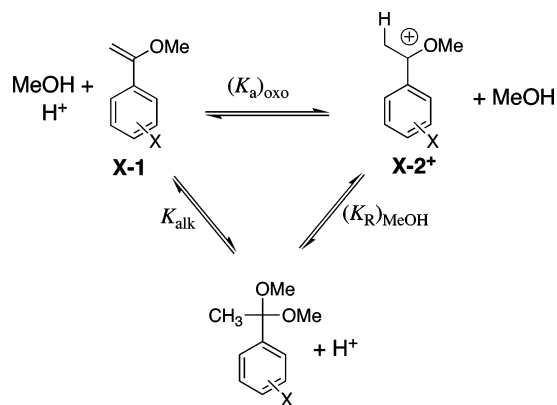
Discussion

We have probed the *extent* of the reversibility of protonation of **H-1** by measuring the yields of the alkene and ketone products that form by deprotonation of **H-2$^+$** generated by acid-catalyzed cleavage of the ketal **H-3** (Scheme 2). The slope of Figure 5 shows that **H-2$^+$** generated in the presence of 1.0 M AcO$^-$ at pH 7 is deprotonated about once for every 300 times that it undergoes nucleophilic addition of water ($k_{AcO}/k_s = 0.0034$ M^{-1}, Scheme 2). Similarly, the intercept of the inset to

(35) Hine, J. *Structural Effects on Equilibria in Organic Chemistry*; Wiley-Interscience: New York, 1975; p 66.

Table 3. Structure−Reactivity Coefficients for Acid-Catalyzed Protonation of **X-1** and Absolute Rate Constants k_s (s^{-1}) for Addition of Water to the Oxocarbenium Ion Reaction Intermediate **X-2$^+$** for Reactions at 25 °C and I = 1.0 (KCl)

ring substituent	k_s/s^{-1}	ΔG°_{av} [a]	α [b,c]	$\partial\alpha/\partial\Delta G^{\circ}_{av}$ [c,d]	carboxylic acid	ΔG°_{av} [a]	β [e]	$\partial\alpha/\partial\Delta G^{\circ}_{av}$ [c,f]
4-MeO-	3.5×10^6	2.7	0.67 ± 0.04	0.0113 ± 0.0041	Cl$_2$CHCO$_2$H	5.4	0.632 ± 0.0028	0.0114 ± 0.0026
H	5×10^7	5.7	0.74 ± 0.03		CNCH$_2$CO$_2$H	7.0	0.667 ± 0.019	
4-NO$_2$	9×10^8	8.8	0.78 ± 0.03		ClCH$_2$CO$_2$H	7.6	0.660 ± 0.021	
3,5-di-NO$_2$	1.4×10^{10}	11.7	0.77 ± 0.03		MeOCH$_2$CO$_2$H	8.0	0.676 ± 0.038	
					CH$_3$CO$_2$H	10.2	0.689 ± 0.027	

[a] The average change in ΔG°, calculated from the data in Table 2. [b] The Brønsted coefficient, determined as the slopes of the correlations shown in Figure 7A. [c] The quoted error is the standard deviation of the slope determined by linear least-squares analysis. [d] The second-derivative structure−reactivity coefficient, calculated as the slope of the correlation shown in Figure 7B. [e] The Brønsted coefficient, determined as the slopes of the correlations shown in Figure 6A. [f] The second-derivative structure−reactivity coefficient, calculated as the slope of the correlation shown in Figure 6B.

Figure 5 shows that **H-2$^+$** is deprotonated by water in an unbuffered solution about once for every 18,000 times that it undergoes nucleophilic addition of water ($k_{HOH}/k_s = 5.5 \times 10^{-5}$). We conclude that deprotonation of **H-2$^+$** is a very rare event in comparison with nucleophilic addition of water. This reflects the larger Marcus intrinsic kinetic barrier to deprotonation compared to that of nucleophilic addition of water.[36]

Lifetimes of Reaction Intermediates. Young and Jencks have studied the specific acid-catalyzed reactions of **4-Me-1** and 4-methylacetophenone dimethyl ketal in the presence of sulfite dianion.[31] Each reaction in the presence of a specified [SO$_3^{2-}$] gives the same yield of sulfite adduct, with rates that are zero-order in [SO$_3^{2-}$]. This shows that these substrates undergo acid-catalyzed reactions through the common intermediate **Me-2$^+$** that is trapped by addition of SO$_3^{2-}$. Absolute rate constants k_s (s^{-1}) for addition of solvent to **X-2$^+$** were estimated from the product rate constant ratios k_{SO3}/k_s and k_{SO3} = 5×10^9 M^{-1} s^{-1} for diffusion-limited addition of sulfite to **X-2$^+$**. These rate constants were revised when it was determined that k_{SO3} is 2-fold smaller than the rate constant for a diffusion-controlled reaction.[34] Rate constants for addition of water to **4-NO$_2$-2$^+$** and to **3,5-di-NO$_2$-2$^+$** estimated using log k_s = 7.7 for the reaction of **H-2$^+$**,[31] the Hammett reaction constant of ρ^+ = 1.6 for addition of water to **X-2$^+$**,[31] and the appropriate Hammett substituent constant σ are reported in Table 3.[35]

The rate constant of k_s = 1.4×10^{10} s^{-1} estimated for the reaction of **3,5-di-NO$_2$-2$^+$** is below the limiting rate constant of 1×10^{11} s^{-1} for a reaction whose rate is controlled by reorganization of the solvation shell that surrounds **3,5-di-NO$_2$-2$^+$** but is similar to that for diffusional steps.[37−41] Therefore, solvent in the initial solvation shell is predicted to react with **3,5-di-NO$_2$-2$^+$** at a rate competitive with diffusion-controlled exchange of solvent from this shell with other nucleophiles. The largest rate constant for deprotonation of **X-2$^+$** by an alkane carboxylate ion estimated in this work is k_A = 5×10^6 M^{-1} s^{-1} for deprotonation of **3,5-di-NO$_2$-2$^+$** by CH$_3$CO$_2^-$ (Table 2). This is far below the diffusion-controlled limit of 5×10^9 M^{-1} s^{-1}. We conclude that there is a chemical barrier to deprotonation of all of these α-methyl oxocarbenium ions by added buffer anions. A value of k_{HO} = 1.5×10^{10} M^{-1} s^{-1} for deprotonation of **4-MeO-2$^+$** by hydroxide ion can be calculated from k_w = 3.1×10^{-4} s^{-1} for protonation of **4-MeO-1** (Table

(36) Richard, J. P.; Williams, K. B.; Amyes, T. L. *J. Am. Chem. Soc.* **1999**, *121*, 8403−8404.
(37) Giese, K.; Kaatze, U.; Pottel, R. *J. Phys. Chem.* **1970**, *74*, 3718−3725.
(38) Kaatze, U. *J. Chem. Eng. Data* **1989**, *34*, 371−374.
(39) Kaatze, U.; Pottel, R.; Schumacher, A. *J. Phys. Chem.* **1992**, *96*, 6017−6020.
(40) Paradisi, C.; Bunnett, J. F. *J. Am. Chem. Soc.* **1985**, *107*, 8223−8233.
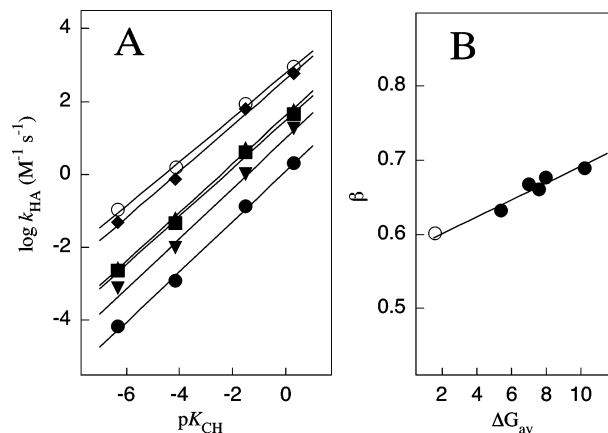(41) Toteva, M. M.; Richard, J. P. *J. Am. Chem. Soc.* **1996**, *118*, 11434−11445.

Figure 6. (A) Brønsted correlations of second-order rate constants log k_{HA} (M^{-1} s^{-1}) for protonation of **X-1** in water at constant ionic strength of 1.0 maintained with KCl. The slope of these plots is equal to the Brønsted coefficient β for proton transfer. Key: (●): Acetic acid catalyst. (▼): Methoxyacetic acid catalyst. (■): Chloroacetic acid catalyst. (▲): Cyanoacetic acid catalyst (♦), dichloroacetic acid catalyst. (○): Hydronium ion catalyst. (B) Change in the Brønsted coefficient β for protonation of **X-1** with changing thermodynamic driving force. The solid line is the least-squares fit determined using data for carboxylic acid catalysts.

1), $(K_a)_{oxo}$ = 0.50 M for deprotonation of **4-MeO-2$^+$** by water, and the relationship k_{HO} = $(k_w)(K_a)_{oxo}/K_w$. This provides evidence that there is little or no chemical barrier to this proton-transfer reaction, which is downhill by almost 20 kcal/mol.

Brønsted Correlations. Linear free-energy relationships between rate and equilibrium constants are an invaluable tool for the study of organic reaction mechanisms. The reactions examined here were chosen because they provide for a large ~15 kcal/mol range of driving force for proton transfer by making small changes in the structure of the reactants at site(s) distant from that for proton transfer. The minimal changes, with changing reaction driving force, in the interaction between the acid catalyst and carbon base reduces the ambiguity in the interpretation of the structure−reactivity correlations reported here.

Figure 6A shows Brønsted correlations of second-order rate constants log k_{HA} (M^{-1} s^{-1}) for general acid-catalyzed hydrolysis of **X-1** by rate-determining protonation of **X-1** (Scheme 1), where the relative basicity of the α-methoxystyrene **X-1** (Table 2) is plotted on the x-axis. The slopes of these correlations for the reactions catalyzed by different carboxylic acids are reported in Table 3 as the Brønsted coefficients β. Figure 7A shows related Brønsted correlations of second-order rate constants log k_{HA} (M^{-1} s^{-1}) for general acid-catalyzed hydrolysis of **X-1** by a group of alkane carboxylic acid catalysts. The slopes of these
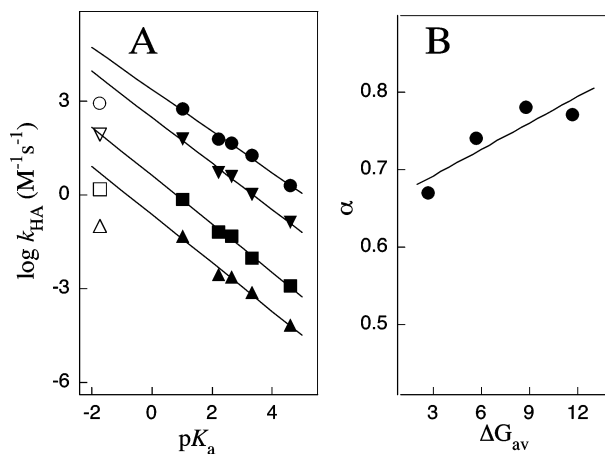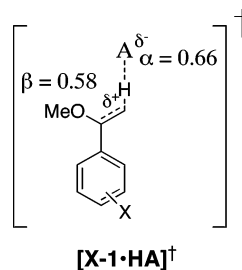
Figure 7. (A) Brønsted correlations of second-order rate constants log k_{HA} (M^{-1} s^{-1}) for protonation of **X-1** in water at constant ionic strength of 1.0 maintained with KCl. The slope of these plots is equal to the Brønsted coefficient α for proton transfer. Key: (●): X = 4-MeO-. (▼): X = H-. (■): X = 4-NO₂-. (▲): X = 3,5-di-NO₂-. Open symbols are for the reactions catalyzed by H_3O^+. (B) The change in the Brønsted coefficient α for protonation of **X-1** with changing thermodynamic driving force.

correlations for the reactions of different **X-1** are reported in Table 3 as the Brønsted coefficients α.

The Brønsted coefficients for chemical reactions provide a measure of the effect of changing polar substituents on the equilibrium constant for a reference chemical reaction—where there is a full unit change in the charge on proceeding from reactant to product—relative to the substituent effect on the rate constants for a second chemical reaction such as protonation of **X-1**.[42] A Brønsted coefficient of close to 1.0 would show that the change in effective charge "seen" by the polar substituent on proceeding from reactant to transition state is similar to the unit change in charge for the reference reaction. A Brønsted coefficient of close to 0.0 shows that there is little or no change in this effective charge on proceeding to the transition state, while intermediate Brønsted coefficients are consistent with partial proton transfer at the transition state.[42] The relationship between the magnitude of the Brønsted coefficient and the fractional transfer of the proton on proceeding to the reaction transition state is not known, but a linear correlation between the two quantities is generally assumed. The observation here of a small, but significant increase in the Brønsted coefficients α and β with increasing thermodynamic barrier to protonation of **X-1** is consistent with a shift to a later, more productlike transition state with increased negative charge at the Brønsted acid catalyst and increased positive charge at the carbon base. This corresponds to a normal Hammond-type effect.[43]

Transition-State Imbalance. Figure 6B shows the change in the Brønsted coefficient β with the change in ΔG_{av}°, the arithmetic average of the changes in ΔG° for protonation of four different **1-X** by a single carboxylic acid, and Figure 7B shows the change in the Brønsted coefficient α with the change in ΔG_{av}° for protonation of a single **1-X** by a series for five carboxylic acids. The y-intercepts of 0.66 for Figure 7B and 0.58 for Figure 6B provide estimates of the Brønsted coefficients α and β, respectively, for thermoneutral proton transfer from the acid catalyst to the basic carbon. These coefficients will be

(42) Hupe, D. J.; Jencks, W. P. *J. Am. Chem. Soc.* **1977**, *99*, 451−464.
(43) Hammond, G. S. *J. Am. Chem. Soc.* **1955**, *77*, 334−338.

$$[X\text{-}1\cdot HA]^{\dagger}$$

the same for a *balanced* transition state in which there is equal development of the interaction between the partial negative charge at the carboxylate oxygen and the alkyl substituent(s) and also of the interaction between partial positive charge at the benzylic carbon and the phenyl ring substituent(s).

The imbalance at $[X\text{-}1\cdot HA]^{\dagger}$ shows that the *apparent* transition-state charges at the reacting acid and base are different. We suggest that this is due to a reduction in the destabilizing inductive transition-state interaction between electron-withdrawing phenyl ring substituent(s) and positive charge at the partly cationic benzylic carbon, because of the attenuation of the unfavorable interaction by enhanced stabilizing resonance electron donation from the α-methoxy group. This will increase the charge at the α-methoxy oxygen and the *separation* of this charge from electron-deficient ring substituent(s).[44−46] The resulting reduction in the polar interactions between these centers would cause a decrease in the Brønsted coefficient β relative to α, because α reflects the *normal* expression of polar interactions between substituents at the carboxylic acid and the reacting acidic oxygen. A similar attenuation of the large inductive destabilization of methoxybenzyl carbocations caused by strongly electron-deficient groups at the benzylic carbon (e.g., α-CF₃) provides a relatively simple rationalization for the small effects of these groups on the rate constants for nucleophilic addition to α-substituted 4-methoxybenzyl carbocations.[45−47]

Related imbalances, most substantially larger than the imbalance reported here, have been observed for deprotonation of carbon acids by electronegative bases to form resonance-stabilized carbanions.[17,18] There is good theoretical evidence consistent with the existence of these transition-state imbalances in carbanion-forming reactions[48] and a simple physical explanation for their occurrence.[3,49]

The Second-Derivative Structure−Reactivity Effect. The slope of the least-squares line through the data in Figure 6B is equal to $\partial\beta/\partial\Delta G_{av}^{\circ} = 0.011 \pm 0.0026$ (standard deviation) and the slope of the least-squares line through the data in Figure 7B is equal to $\partial\alpha/\partial\Delta G_{av}^{\circ} = 0.011 \pm 0.0041$ (standard deviation). There is good agreement between the slopes of the correlations from Figures 6B and 7B, as required for these cross-correlation coefficients.[50] The difference in the uncertainty of the slopes of the correlations from Figures 6B and 7B is discussed below. These data are consistent with an earlier estimate of a limit of $\partial\alpha/\partial\Delta G_{av}^{\circ} \leq 0.026$ for protonation of a

(44) Amyes, T. L.; Stevens, I. W.; Richard, J. P. *J. Org. Chem.* **1993**, *58*, 6057−6066.
(45) Richard, J. P. *J. Am. Chem. Soc.* **1989**, *111*, 1455−1465.
(46) Richard, J. P. *Tetrahedron* **1995**, *51*, 1535−1573.
(47) Richard, J. P.; Amyes, T. L.; Bei, L.; Stubblefield, V. *J. Am. Chem. Soc.* **1990**, *112*, 9513−9519.
(48) Bernasconi, C. F.; Wenzel, P. J. *J. Am. Chem. Soc.* **1994**, *116*, 5405−5413.
(49) Kresge, A. J. *Can. J. Chem.* **1974**, *52*, 1897−1903.
(50) Jencks, D. A.; Jencks, W. P. *J. Am. Chem. Soc.* **1977**, *99*, 7948−7960.
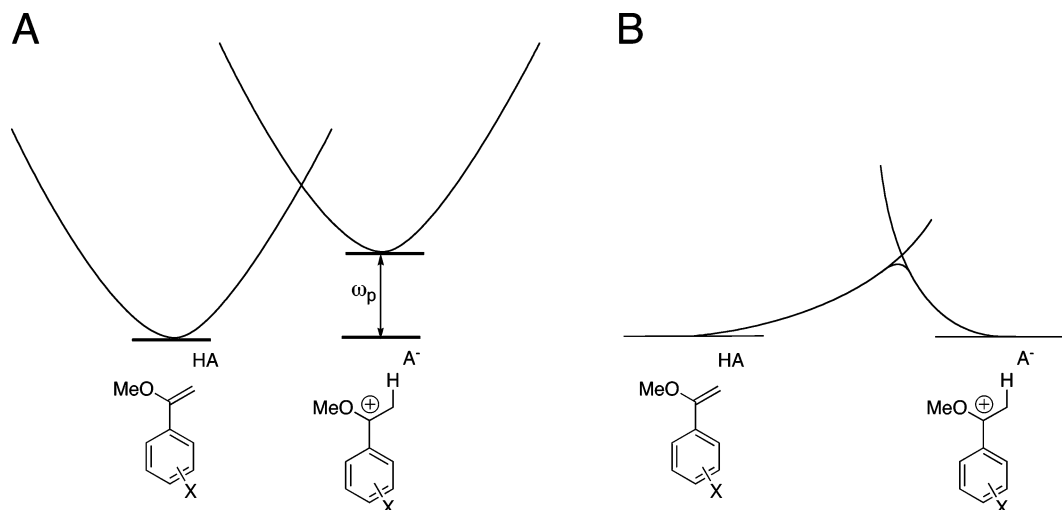
Figure 8. Two hypothetical reaction profiles which might be used to rationalize the observation of a relatively late transition state for thermoneutral protonation of **X-1** by alkane carboxylic acids. (A) Reaction profile for which the chemical barrier to the proton-transfer step is uphill, but the overall reaction is thermoneutral, because the negative work associated with the breakdown of the product complex (ω_p) is greater than the positive work associated with the formation of the reactant complex ($\omega_r \approx 0$). (B) Asymmetric reaction profile which shows a shallow curvature close to the reactants and a much steeper curvature close to the products.

more structurally diverse series of vinyl ethers.[51]

$$\log k_o = 12.8 - \Lambda/1.36 \qquad (11)$$

The slopes $\partial\alpha/\partial\Delta G^\circ_{av} = \partial\beta/\partial\Delta G^\circ_{av} = 1/8\Lambda = 0.011$ of the correlations from Figures 6B and 7B are consistent with an intrinsic barrier of 11 kcal/mol for a reaction coordinate that can be described by Marcus theory (eqs 1–3). The range of intrinsic barriers consistent with these data is 8–18 kcal/mol, calculated for the larger error limit of ± 0.0041. By comparison, a value of $\Lambda = 13$ kcal/mol can be calculated from the intrinsic rate constant of $\log k_o$ (M^{-1} s^{-1}) = 3.2 for protonation of **4-MeO-1** by using eq 11. This intrinsic rate constant was determined by making a short linear extrapolation to $\Delta G^\circ = 0$ of a plot of $\log k_{HA}$ against ΔG°. We conclude that these data are consistent with a reaction in which there is little work done on reactants in the formation of the reaction complex so that $\omega_r \approx \omega_P \approx 0$ (eq 1) for formation of a complex similar to that formed by simple diffusional encounter of **1-X** and carboxylic acid catalysts.

Two other effects, in addition to a formal shift in the position of the reaction transition state, may contribute to the observed value of $\partial\alpha/\partial\Delta G^\circ_{av} = \partial\beta/\partial\Delta G^\circ_{av} = 0.011$.

(1) There may a change in these Brønsted coefficients that *opposes* the change from a Hammond-type shift in the structure of the transition state that arises from changing electrostatic interactions between substituents at the vinyl ether and the carboxylic acid reactants.[52–54] For example, the interaction between the electron-deficient 3,5-nitro groups at **3,5-di-NO₂-1** and electron-rich or electron-deficient groups at the carboxylic acid catalyst are stabilizing ($\uparrow k_{HA}$) and destabilizing ($\downarrow k_{HA}$), respectively, compared to the interactions with the hydrogen at **4-H-1**. Such a change in rate constants for weakly and strongly acidic catalysts will have the effect of causing a *decrease* in the Brønsted coefficient α. The value of $-(\partial\alpha/\partial K_{BH}) = -0.013$

determined for the electrostatic cross-correlation coefficient ($-\tau$) in studies on the formation of hydrogen bonds between substituted phenoxide anions and alkane ammonium ions in water[54] suggests that such electrostatic effects may mask a change in structure–reactivity coefficients for protonation of vinyl ethers that arise from a shift in the position of the reaction transition state.

(2) The difference in the uncertainty of the slopes of the correlations shown in Figure 6B ($\partial\beta/\partial\Delta G^\circ_{av} = 0.011 \pm 0.0026$) and in Figure 7B ($\partial\alpha/\partial\Delta G^\circ_{av} = 0.011 \pm 0.0041$) reflects the *apparent* downward curvature for the latter correlation. Such *apparent* curvature may simply be due to the uncertainty in the experimental data. However, the curvature is caused mainly by the large 0.07 unit change in α for the 4-OMe for 4-H substitution at **X-1** (Table 3); and this large change may be observed because the strongly resonance electron-donating 4-MeO- group causes a significant increase in the Marcus intrinsic reaction barrier Λ compared to the reaction of other **X-1**,[55] similar to the exalted value of Λ observed for deprotonation of the 1-(4-methoxyphenyl)ethyl carbocation.[56] Such a specific increase in Λ for protonation of **4-MeO-1** would cause a decrease in α that reflects the tendency of reactions with very large intrinsic barriers to react through central transition states with $\alpha = \beta = 0.50$. This would correspond to a third-derivative structure–reactivity effect.[33] These effects have been extensively documented for related reactions.[8,23,33,57] The effect would cause the observed value of $\partial\alpha/\partial\Delta G^\circ_{av} = \partial\beta/\partial\Delta G^\circ_{av} = 0.011$ to overestimate the shift in the position of the transition state from a Hammond effect and would compensate for any opposing contribution of the electrostatic term τ discussed above.

The following Marcus parameters for protonation of vinyl ethers by hydronium ion have been reported in earlier work: (1) $\Lambda = 4$ kcal/mol, $\omega_r = 13$ kcal/mol, and $\omega_P = 11$ kcal/mol, obtained from the very poorly defined fit of a small set of six rate constants for protonation of **X-1** by H_3O^+ to an equation that contains three variable parameters[21] and (2) $\Lambda = 4$ kcal/mol and $\omega_r = 10$ kcal/mol that were obtained by an analysis of the change in the solvent kinetic deuterium isotope effect with changing vinyl ether reactivity for lyonium-ion catalyzed

(51) Murray, C. J.; Jencks, W. P. *J. Am. Chem. Soc.* **1990**, *113*, 1880–1889.
(52) Hine, J. *J. Am. Chem. Soc.* **1972**, *94*, 5766–5771.
(53) Rothenberg, M. E.; Richard, J. P.; Jencks, W. P. *J. Am. Chem. Soc.* **1985**, *107*, 1340–1346.
(54) Stahl, N.; Jencks, W. P. *J. Am. Chem. Soc.* **1986**, *108*, 4196–4205.

hydrolysis of a broad range of vinyl ethers.[29] This second analysis was carried out in the absence of the determination of the thermodynamic driving force $\Delta G°$ for proton transfer to form the oxocarbenium ion.[58] A value of $\Lambda = 4$ kcal/mol requires a cross correlation coefficient of $\partial\alpha/\partial\Delta G°_{av} = \partial\beta/\partial\Delta G°_{av} = 0.031$ that is substantially larger than the value of 0.011 determined in this work. We conclude that if there is a sharp change in the position of the transition state for a reaction with $\Lambda = 4$ kcal/mol, then the effect of this change on the observed Brønsted coefficients α and β is masked by a large electrostatic term τ that causes an opposing change in the magnitude of these coefficients (see above).

Thermoneutral Proton Transfer. The *y*-intercepts of 0.66 for Figure 7B and of 0.58 for Figure 6B are equal to the Brønsted coefficients α and β, respectively, when $\Delta G° = 0$ for proton transfer from the acid catalyst to the basic carbon. These Brønsted coefficients are both greater than the value of $\alpha = \beta = 0.50$ predicted by Marcus theory for thermoneutral proton transfer.[7] A value of $\alpha > 0.50$ for thermoneutral proton transfer might be explained by one of the two reaction coordinate profiles shown in Figure 8.

(1) The data are consistent with a reaction profile (Figure 8A) in which the chemical barrier to the proton-transfer step is uphill, but the overall reaction is thermoneutral because the negative work associated with the breakdown of the product complex (ω_p) is greater than the positive work associated with the formation of the reactant complex (ω_r). Extrapolation of the correlation from Figure 7B gives $\alpha = 0.50$ when proton transfer to a hypothetical **X-1** is favorable by 14 kcal/mol. For a symmetrical reaction (Figure 8A), this corresponds to 14 kcal/mol greater work done in the formation of the product compared to that for the reactant complex from free species. There may, indeed, be work associated with the desolvation of the product ions RCO_2^- and **X-2**$^+$ when they are brought together to form the reaction complex, but part or all of this may be "recovered"

as stabilizing electrostatic interactions between the oppositely charged ions. In any case, we are not able to offer a physical explanation for any large *difference* in the respective work done to form reactant and product complexes and consider this to be unlikely explanation for the large Brønsted coefficients observed for thermoneutral proton transfer.

(2) The exalted value of α for thermoneutral proton transfer is consistent with a smaller curvature along the free-energy surface near the reactants, where the primary motion is stretching of the O—H bond of a carboxylic acid, compared with the energy surface near the products, where the primary motion is stretching of the C—H bond of the α-alkoxy carbocation (Figure 8B). Such an asymmetric reaction coordinate is in keeping with the notion that it may be constructed as a hybrid of (a) the energy surface close to the reactants, which is dominated by proton transfer at oxygen and shows shallow curvature expected for a reaction with a small intrinsic barrier[59] and (b) the energy surface near the products, which is dominated by proton transfer at carbon and shows steep curvature expected for this reaction with a large intrinsic barrier.[17,18]

Concluding Remarks

This discussion collides with the limits of what might be learned about the transition-state structure and reaction coordinate profile for protonation of **X-1** from systematic analyses of rate−equilibrium relationships. These limits are best extended through computational studies, which reproduce experimental structure−reactivity coefficients and provide additional insight into questions that are not easily resolved by experiment.

Supporting Information Available: Details of procedures for the synthesis of 4-methoxyacetophenone dimethyl ketal, acetophenone dimethyl ketal, 4-nitroacetophenone dimethyl ketal, 3,5-dinitroacetophenone dimethyl ketal, α-methoxy-4-methoxystyrene, α-methoxystyrene, α-methoxy-4-nitrostyrene, and α-methoxy-3,5-dinitrostyrene; Tables S1−S7 of observed first-order rate constants (k_{obsd}) for hydrolysis of **X-1** in solutions that contain HCl or carboxylic acids. This material is available free of charge via the Internet at http://pubs.acs.org.

JA071007K

(55) Any effect which causes a change in the Brønsted coefficient for the reaction of **4-MeO-1**, such as a change in the intrinsic reaction barrier or a change to a concerted reaction mechanism, will be very difficult to detect as curvature that is caused by the change in the position of a single data point on the correlations shown in Figure 6A. This effect will be easier to detect on the correlations shown in Figure 7A, because all of the deviant rate constants are present on the single Brønsted correlation for the reaction of the deviating compound **4-MeO-1**.

(56) Richard, J. P.; Amyes, T. L.; Lin, S. S.; O'Donoghue, A. C.; Toteva, M. M.; Tsuji, Y.; Williams, K. B. *Adv. Phys. Org. Chem.* **2000**, *35*, 67−115.

(57) Sørenson, P. E.; Jencks, W. P. *J. Am. Chem. Soc.* **1987**, *109*, 4675−4690.

(58) The value of the Brønsted coefficient β for protonation of **X-1** by H_3O^+ lies on the correlation between β and reaction driving force determined for protonation of **X-1** by carboxylic acids (Figure 6B). This provides evidence that there is not a large difference in the value of intrinsic barrier Λ for the reaction of these different types of Brønsted acids.

(59) Eigen, M. *Angew. Chem., Int. Ed. Engl.* **1964**, *3*, 1−72.